Available online at www.sciencedirect.com
SCIENCE DIRECT®
Journal of Power Sources 115 (2003) 229–235
JOURNAL OF POWER SOURCES
www.elsevier.com/locate/jpowsour

Catalysts for direct formic acid fuel cells

C. Rice[a], S. Ha[a], R.I. Masel[a,*], A. Wieckowski[b]

[a]*Department of Chemical Engineering, University of Illinois, Roger Adams Laboratory, P.O. Box C3, 600 South Mathews Avenue, Urbana, IL 61801, USA*
[b]*Department of Chemistry, University of Illinois, Urbana, IL 61801, USA*

Received 9 December 2002; accepted 18 December 2002

Abstract

Previous work has demonstrated that formic acid fuel cells show interesting properties for micro power generation. In this paper the effects of the anode catalyst composition on fuel cell performance is investigated. In particular, the performance of Pt, Pt/Pd and Pt/Ru catalysts for direct formic acid fuel cells is investigated and their effect on cell power density output at 30 °C are compared. It is found that the open cell potential varies significantly with the catalyst composition. The Pt/Pd catalyst shows an open cell potential of 0.91 V compared to 0.71 V with pure platinum and 0.59 V with Pt/Ru. The current at a cell potential of 0.5 V is 62 mA/cm^2 with Pt/Pd compared to 33 mA/cm^2 with pure platinum and 38 mA/cm^2 with Pt/Ru. Interestingly, the Pt/Ru catalyst gives the most power at low voltage 70 mW/cm^2 at 0.26 V, compared to 43 mW/cm^2 for pure platinum and 41 mW/cm^2 for Pt/Pd. All of the catalysts showed stable operation during several hour tests. Analysis of the data indicates that the addition of palladium enhances the rate of formic acid electrooxidation via a direct reaction mechanism, while ruthenium additions suppress the direct pathway and enhance electrooxidation via a reactive CO intermediate.

Keywords: Formic acid; Catalyst; Fuel cell

1. Introduction

In recent papers, we have shown that direct formic acid polymer electrolyte membrane (PEM) fuel cells have interesting properties for micro power generation [1,2]. Formic is a liquid at room temperature and a reasonable electrolyte. Direct formic acid-oxygen fuel cells have a high theoretical open circuit potential i.e. emf (1.45 V), limited fuel crossover, and reasonable power densities at room temperature [4]. Formic acid being a relatively strong electrolyte facilitates proton transport within the anode compartment of the PEM fuel cell. Fuel crossover from the anode to the cathode is small, because of anodic repulsion between the Nafion® and the partially dissociated form of formic acid (formate anions) [4,5]. While formic acid has a lower power density than methanol, only 1740 W h/kg, one can run the fuel cell with 20 M (70% by weight) solutions. Consequently, the fuel cells are quite competitive on a fuel power density basis.

In this paper, the effects of the anode catalyst composition on fuel cell performance are carefully investigated. In particular, the performance of Pt, Pt/Pd and Pt/Ru catalysts for direct formic acid fuel cells are investigated and their effect on cell power density output at 30 °C are compared.

To put this work in perspective, note that the electrooxidation of formic acid is thought to occur via two parallel pathways [6–12]. In the ''direct pathway'', the formic acid is directly oxidized to form CO_2 without forming a carbon monoxide intermediate

$$HCOOH + Pt^0 \rightarrow X \rightarrow CO_2 + 2H^+ + 2e^- \quad (1)$$

In the ''CO pathway'', the formic acid first reacts to form a CO intermediate, then the CO is oxidized to CO_2

$$HCOOH + Pt^0 \rightarrow Pt{-}CO + H_2O \quad (2)$$

$$Pt^0 + H_2O \rightarrow Pt{-}OH + H^+ + e^- \quad (3)$$

$$Pt{-}CO + Pt{-}OH \rightarrow 2Pt^0 + CO_2 + H^+ + e^- \quad (4)$$

$$\text{overall}: HCOOH \Rightarrow CO_2 + 2H^+ + 2e^- \quad (5)$$

Previous studies in an electrochemical cell have shown that the rate of formic acid electrooxidation on pure platinum is insufficient for practical fuel cells. Palladium additions to a platinum catalyst enhance reaction 1 [17] while ruthenium would be expected to enhance reaction 4. The mechanism

* Corresponding author. Tel.: +1-217-3336841; fax: +1-217-3335052.
E-mail address: r-masel@uiuc.edu (R.I. Masel).

0378-7753/03/$ – see front matter
doi:10.1016/S0378-7753(03)00026-0

of the enhancement has not yet been determined, but for an analogous system, methanol oxidation, the addition of Ru onto Pt enhances the activation of water at low potentials, through the so-called bifunctional mechanism, thereby increasing the overall rate of oxidation via CO removal [13–16].

The purpose of the present work is to compare the behavior of platinum black, platinum-ruthenium and platinum-palladium under real fuel cell conditions to see whether the observations from the electrochemical cells apply to real fuel cell operating conditions.

2. Experimental

The membrane electrode assemblies (MEAs) were fabricated using a 'direct paint' technique to apply the catalyst layer. The active cell area is 5 cm^2. The 'catalyst inks' were prepared by dispersing the catalyst nanoparticles into appropriate amounts of deionized water and a 5% recast Nafion® solution (1100 EW, from Solution Technology, Inc.). Then both the anode and cathode 'catalyst inks' were directly painted onto either side of a Nafion® 117 membrane. For all MEAs prepared in this study, the cathode consisted of unsupported platinum black nanoparticles (27 m^2/g, Johnson Matthey) at a standard loading of 7 mg/cm^2. The anode consisted of catalyst particles at a standard loading of 4 mg/cm^2 (27 m^2/g). A carbon cloth diffusion layer (E-Tek) was placed on top of both the cathode and anode catalyst layers. Both sides of the cathode side carbon cloth, were Teflon®-coated for water management. A single-cell test fixture consisted of machined graphite flow fields with direct liquid feeds and gold plated copper plates too avoid corrosion (Fuel Cell Technologies Inc).

Three distinct anode catalysts were investigated in this study: (i) "Pt", platinum black (Johnson Matthey); (ii) "Pt/Ru", platinum black modified by a submonolayer of spontaneously deposited Ru [19], and [3]) "Pt/Pd" platinum black modified by a submonolayer of spontaneously deposited Pd. The spontaneous deposition process is described in detail in Waszczuk, et al. [18]. The process starts with Johnson Matthey Hispec 1000 platinum black. The platinum black is cleaned by cyclic voltametry, and then a metal salt, $RuCl_3$ or $Pd(NO_3)_2$, is adsorbed onto the platinum black's surface. Then, the solution containing metal salt is removed, and the sample is further cleaned using cyclic voltametry. Generally, two deposition cycles were used in the experiments here. The Pt/Pd catalyst had a platinum core with about 60% of the platinum surface covered by palladium while the Pt/Ru catalyst had a platinum core with about 40% of the platinum surface covered by ruthenium. The Pt, Pt/Ru and Pt/Pd catalysts all had specific surface areas of about 27 m^2/g respectively.

During the experiments reported in this paper, the MEAs were initially conditioned at room temperature within the test fixture with methanol/humidified H_2 (10 °C above cell temperature; fuel cell anode/cathode) by running several anode polarization curves, while slowly increasing to a final cell temperature of 80 °C. The fuel cell cathode acted as a dynamic hydrogen reference electrode (DHE), as well as a high surface area counter electrode during this conditioning process, the H_2 flow rate was 100 cm^3 under a 10 psig backpressure, the gas stream was humidified to 10 °C above cell temperature. Methanol (1 M) was supplied to the anode side of the fuel cell MEA, at a flow rate of 0.5 ml/min and acted as the working electrode for an electrochemical cell. The anode potential was controlled with a power supply (Hewlett-Packard, model 6033 A) the potential was stepped in 10 mV increments at 5 s intervals.

The MEA was further conditioned at 80 °C while supplying H_2/O_2 to the anode/cathode in the fuel cell mode, while holding the cell potential at 0.6 V for 1–2 h. The cell potential was controlled with a fuel cell testing station (from Fuel Cell Technologies Inc. The H_2 flow rate was set to 200 cm^3, the gas stream was humidified to 95 °C prior to entering the cell, and a backpressure of 30 psig was applied. The O_2 flow rate was 100 cm^3, the gas stream was humidified to 90 °C, and a backpressure of 30 psig was applied. After conditioning with H_2/O_2 the cell temperature was lowered to 30 °C. A cell polarization curve with 4 M methanol (0.5 ml/min)/O_2 (100 cm^3, 40 °C) was acquired as the final conditioning step [20].

Cell polarization curves were obtained on each of the different anode catalyst MEAs at 30 °C with 5 M formic acid (Aldrich, 96% A.C.S. grade) at a flow rate of 0.5 ml/min. O_2 was supplied to the cathode at a flow rate of 100 cm^3 under 30 psi of backpressure, humidified to 40 °C.

Constant voltage tests were performed at 0.6, 0.5, 0.4 and 0.3 V in 5 M formic acid at a flow rate of 0.2 ml/min. O_2 was supplied to the cathode at a flow rate of 100 cm^3 under 30 psi of backpressure, humidified to 40 °C. The potential load was initially applied by stepping from the open circuit potential to 0.1 V, then to the desired applied potential.

Carbon monoxide (CO) stripping cyclic voltammograms were acquired at 30 °C. The anode functioned as a working electrode during the measurements; the potential was controlled with a potentiostat/galvanostat (Solartron, model SI 1287), at a scan rate of 1 mV/s. H_2 was fed to the fuel cell cathode compartment, the platinum/H_2 combination acted as a dynamic reference electrode and as a counter electrode. The H_2 flow rate was 100 cm^3, under a constant backpressure of 10 psig, humidified to 40 °C. During CO adsorption the anode potential was held at 0.15 V versus DHE. Initially, argon (Ar) was supplied to the fuel cell anode: 400 cm^3, backpressure 30 psig, humidified to 40 °C. CO was adsorbed onto the surface from 0.1% CO in Ar (at 400 cm^3, backpressure 30 psig, humidified to 40 °C) for 30 min. The compartment was then flushed for 10 min with Ar. The surface area for each anode was determined from the CO stripping peak, assuming a packing density equal to 1.0.

3. Results

Fig. 1A illustrates the effect of anode catalyst composition on the cell polarization curve profile. Three distinct precious metal catalysts were tested: platinum black (Pt); ruthenium doped platinum black (Pt/Ru); and Pd doped Pt black (Pt/Pd). Note that the open circuit potential was catalyst dependent: the open cell potential is 0.71 V with a platinum anode and the open circuit potential decreases to 0.59 V when ruthenium is added to the platinum anode catalyst. By contrast, the open circuit potential increases to 0.91 V when palladium is added to the anode catalyst. With the Pt/Pd catalyst there is a substantial current density output below 0.8 V, unlike the Pt and Pt/Ru anode catalysts, for which current is not observed until the applied voltage is below 0.6 V. Interestingly, larger current densities were observed in the reverse scan for both Pt and Pt/Pd. For the Pt/Ru catalyst, the forward and reverse scans are basically identical. At 0.5 V on the reverse scan the current density output for the three anode catalysts are: Pt (33 mA/cm^2); Pt/Ru (38 mA/cm^2); and Pt/Pd (62 mA/cm^2). However, Pt/Ru has the highest current density at the highest loadings (lower applied potentials). At 0.2 V after scan reversal the current density outputs are: Pt (187 mA/cm^2); Pt/Ru (346 mA/cm^2); and Pt/Pd (186 mA/cm^2).

In Fig. 1B, the results from Fig. 1A are shown as power density versus voltage cell. The maximum power density attained on each of the three catalysts was: Pt 43 mW/cm^2 (0.26 V); Pt/Ru 70 mW/cm^2 (0.26 V); and Pt/Pd 41 mW/cm^2 (0.27 V).

Fig. 2 shows anode polarization curves for each of the catalysts in 5 M formic acid. The anode polarization plots differ from the cell polarization plots, in that the potential of the fuel cell anode compartment is directly referenced against a dynamic reference electrode. This removes the effects of the cathode, thereby facilitating quantitative interpretation of the anode catalyst performance.

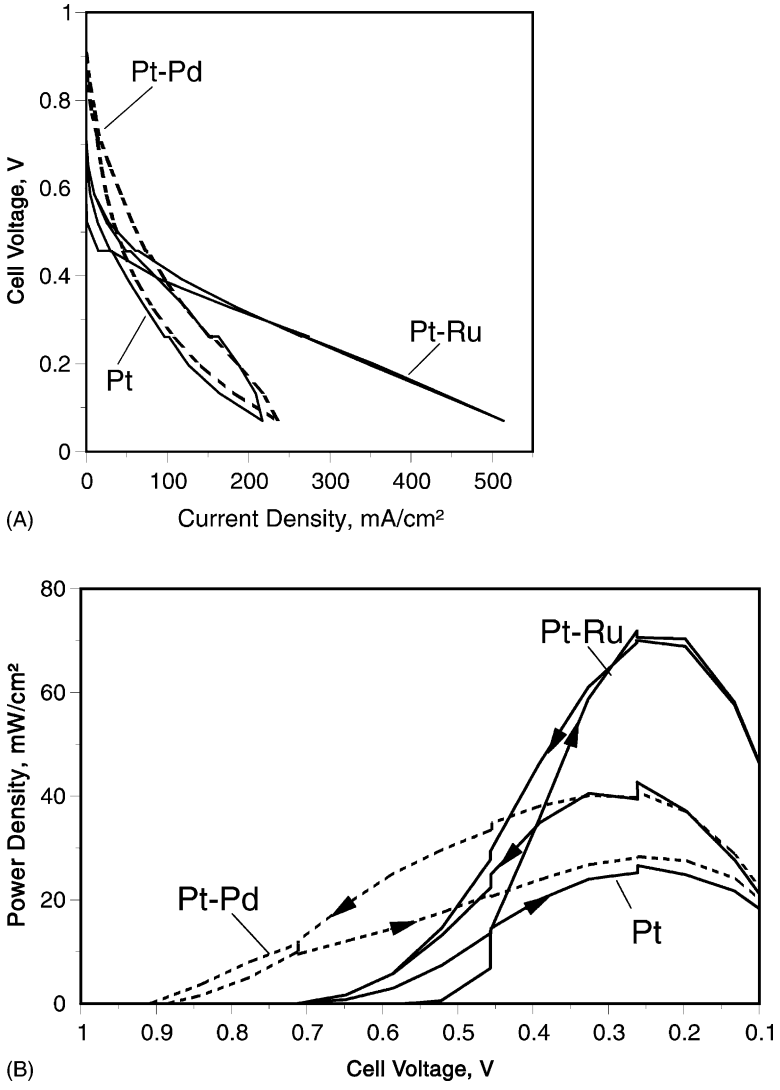

Fig. 1. Formic acid/O_2 current density at 30 °C: (A) cell polarization; and (B) power density curves. The anode was supplied with 5 M formic acid at a flow rate of 0.5 ml/min. Humidified (40 °C) O_2 was supplied to the cathode at a flow rate of 100 cm^3.

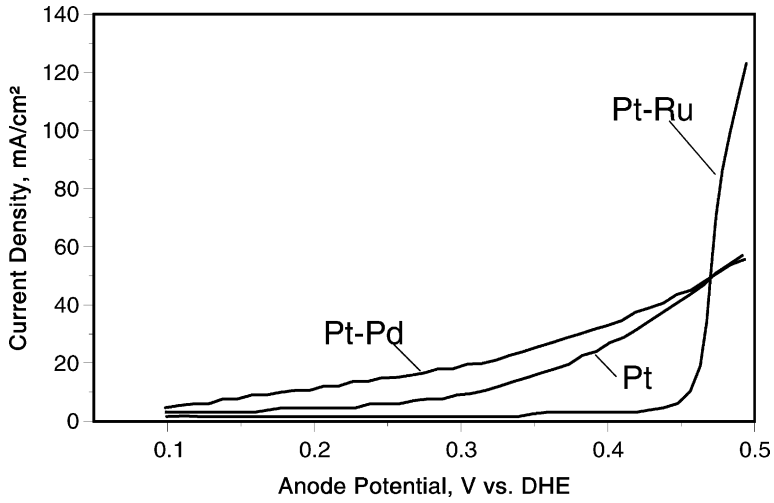

Fig. 2. Anode polarization in 5 M formic acid at a flow rate of 0.5 ml/min on platinum black, Pt/Ru and Pt/Pd; cell temperature, 30 °C. The potential was stepped in 10 mV increments at 5 s intervals, corrected for *iR* drop. The cathode acted as a dynamic hydrogen reference electrode/counter electrode: humidified (40 °C) H_2 was supplied at a flow rate of 100 cm^3.

The anode polarization results reflect those in Fig. 1A. The general curve shape is similar for both Pt and Pt/Pd, a slow steady increase in current density with applied anode potential. There is greater than a 0.1 V difference in the on set of formic acid oxidation on the Pt and Pt/Pd anode catalyst, partially accounting for the 0.2 V difference in the open circuit potential. For the Pt/Ru anode catalyst there is no current density at potentials below 0.4 V versus DHE, followed by a sharp increase in activity above 0.45 V, probably corresponding to the on set of water activation on by Ru.

Table 1 shows the current density at different anode potentials. Again we found that at low loads (high cell potentials) the currents are higher on Pt/Pd than for Pt or Pt/Ru. However, the effect was smaller than reported previously [17] in a conventional three electrode electrochemical cell.

Constant voltage tests were done at applied cell potentials ranging from 0.6 to 0.3 V in Figs. 3–6. In all of the curves there is a sharp initial current drop, followed by a slower decay. In longer runs we found that there continues to be a slow decay in activity for the Pt and Pt/Ru catalyst after several hours, but the current was stable on Pt/Pd after about 2 h.

In Fig. 3 the applied cell potential was 0.6 V. Only the Pt and Pt/Pd catalyst showed appreciable current densities at this applied potential, consistent with the cell polarization curves in Fig. 1.

In Fig. 4 constant voltage tests were run at a cell potential of 0.5 V. An initial decrease in the current density with time was found for all catalysts. The steady-state current density stabilized for all three catalysts within an hour of the potential hold. The final current densities after holding the cell potential at 0.5 V for 2 h was: Pt 22.02 mA/cm^2 (10.30 mW/cm^2); Pt/Ru 35.14 mA/cm^2 (16.44 mW/cm^2); Pt/Pd 46.39 mA/cm^2 (21.71 mW/cm^2).

Fig. 5 shows the results of the constant voltage test run at a cell potential at 0.4 V for 2 h. The final current density after holding the cell potential of 0.4 V for 2 h was:

Table 1
Current densities seen in the anode polarization experiments in Fig. 2

Anode potential vs. DHE (V)	Pt (mA/cm^2)	Pt/Ru (mA/cm^2)	Pt/Pd (mA/cm^2)
0.2	3	1.6	12
0.3	7.6	1.6	18
0.4	19.6	3	31.6
0.49	43.6	111.36	48

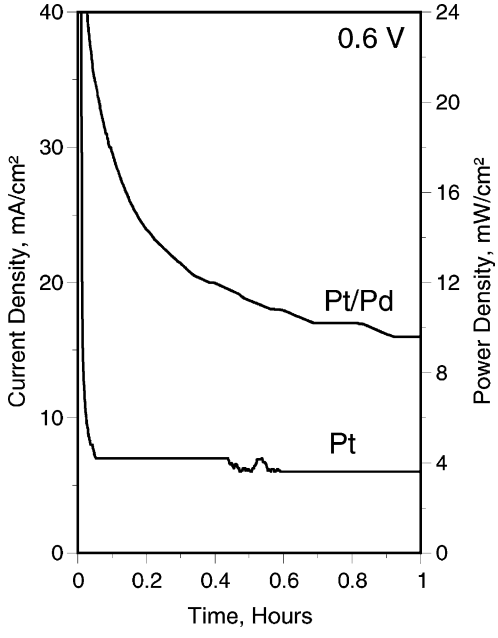

Fig. 3. Constant voltage tests at a cell potential of 0.6 V on Pt and Pt/Pd in 5 M formic acid at 0.2 ml/min. The cell temperature was 30 °C.

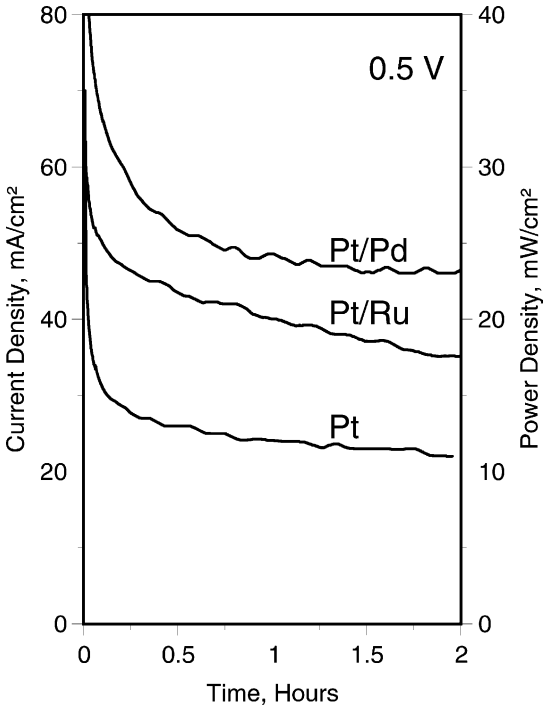

Fig. 4. Constant voltage tests at a cell potential of 0.5 V on platinum black, Pt/Ru, and Pt/Pd in 5 M formic acid at 0.2 ml/min. The cell temperature was 30 °C.

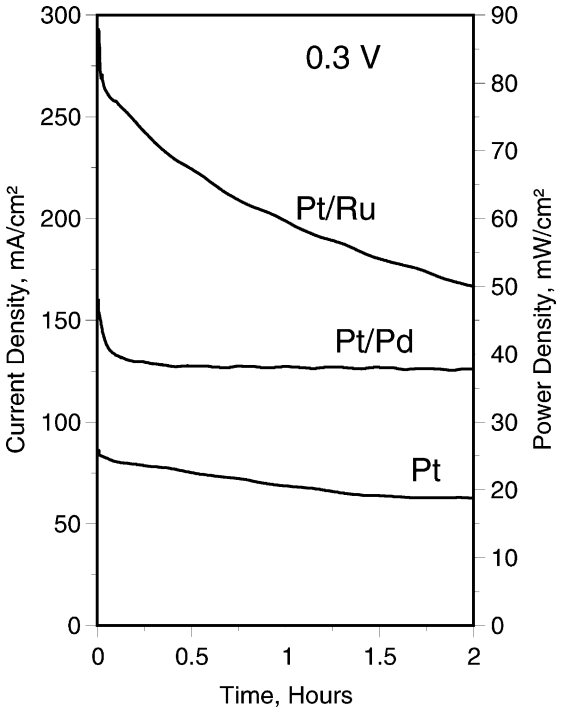

Fig. 6. Constant voltage tests at a cell potential of 0.3 V on platinum black, Pt/Ru, and Pt/Pd in 5 M formic acid at 0.2 ml/min. The cell temperature was 30 °C.

Pt 37.44 mA/cm^2 (15.69 mW/cm^2); Pt/Ru 60.61 mA/cm^2 (25.40 mW/cm^2); Pt/Pd 67.32 mA/cm^2 (28.24 mW/cm^2).

The final constant voltage test was obtained at a cell potential at 0.3 V, Fig. 6. At this applied potential the Pt/Ru catalyst performs the best. The final current densities after holding the cell potential of 0.3 V for 2 h were: Pt 62.53 mA/cm^2 (19.36 mW/cm^2); Pt/Ru 166.72 mA/cm^2 (51.35 mW/cm^2); Pt/Pd 125.98 mA/cm^2 (39.14 mW/cm^2).

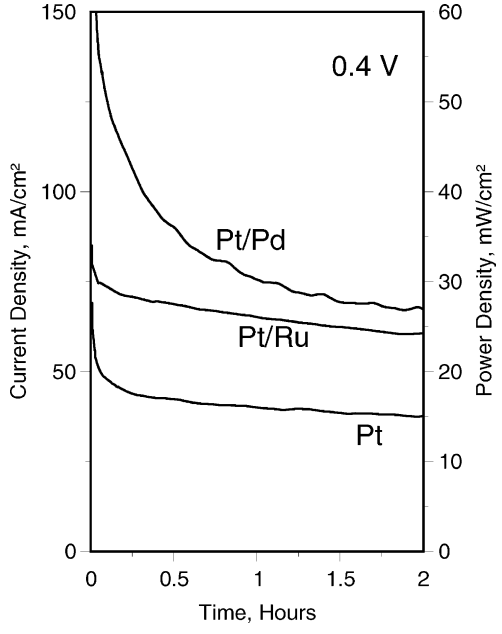

Fig. 5. Constant voltage tests at a cell potential of 0.4 V on platinum black, Pt/Ru, and Pt/Pd in 5 M formic acid at 0.2 ml/min. The cell temperature was 30 °C.

An extended constant voltage test (10 h) was performed on the Pt/Pd anode catalyst at a cell potential of 0.3 V. Within the first hour and a half a steady-state current of 111.43 mA/cm^2 (34.14 mW/cm^2) was reached. The power density fluctuated around an average steady-state value throughout the duration of the experiment once the maximum value was reached, with no decrease in activity.

In order to further elucidate the dominant reaction mechanism for the three anode catalysts, CO stripping cyclic voltammetry was performed. Fig. 7 shows the effect of catalyst type on CO stripping. A weak pre-wave precedes the broad bulk CO stripping peak on Pt at 0.618 V versus DHE. The CO stripping peak on Pt/Ru shows two poorly resolved features, probably corresponding to two adsorbed CO populations, (1) CO adsorbed on or near Ru islands (0.418 V versus DHE) and (2) CO adsorbed on Pt (∼0.47 V versus DHE). Wieckowski and co-workers explain the peak splitting phenomenon in detail in Tong et al. [19]. There is a single sharp peak for CO stripping from the Pt/Pd catalyst at 0.67 V versus DHE.

Notice that the CO stripping peak on Pt/Ru is at a 0.2 V lower potential than the CO stripping peak on Pt. The opposite trend is found for CO stripping from Pt/Pd, there is a 0.052 V increase in the peak potential compared to Pt, indicating an increase in the energy required to remove CO from the catalyst surface. Evidently, the Pt/Pd catalyst is the

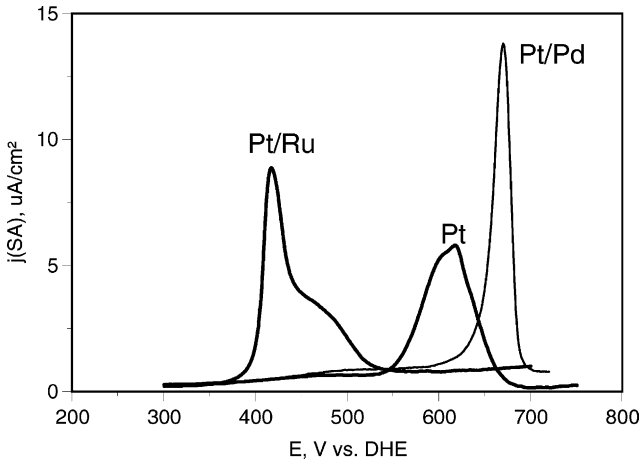

Fig. 7. CO stripping cyclic voltammograms for platinum black, Pt/Ru, and Pt/Pd. The cell temperature was 30 °C. The anode was exposed to 0.1% CO gas in Ar for 30 min, prior to purging with Ar for 10 min. The scan rate was 1 mV/s, in the presence of Ar, 400 cm^3, backpressure 30 psig, humidified to 40 °C. The cathode was set-up as a dynamic hydrogen reference electrode/counter electrode: humidified (40 °C) H_2 was supplied at a flow rate of 100 cm^3.

least active for CO oxidation, even though the Pt/Pd catalyst shows the highest open circuit cell potential and the highest activity for formic acid oxidation at low potentials with respect to DHE.

4. Discussion

The results in Figs. 1–7 show that there are significant differences in the performance of platinum, platinum/palladium and platinum/ruthenium even though all three catalysts have essentially identical surface areas. Fig. 1A shows that the cell with a Pt/Pd anode catalyst shows a 0.2 V higher open circuit potential than the cells with either Pt or Pt/Ru as the anode catalyst. The trends for the forward and reverse scans for both Pt and Pt/Pd are similar. There is an enhancement in the measured current density upon reversal of the scan, possibly linked to an increase in activity by stepping to a lower cell potential. For the Pt/Ru anode catalyst the forward and reverse cell polarization scans are the same.

Pt/Pd produces higher current densities within the operating range of interest for a fuel cell (cell potentials of 0.7–0.45 V) leading to higher overall cell efficiencies. At a cell potential of 0.5 V there is about an 80% increase in activity over that of either the Pt or Pt/Ru anode catalyst. At lower cell potentials the Pt and Pt/Pd performance is similar. The Pt/Ru catalyst performs best at cell potentials below 0.4 V. At a cell potential of 0.2 V: Pt/Ru is 2.5 times more active than either of the other two catalysts. Fig. 1B further organizes the results in Fig. 1A in terms of the power density.

It is interesting to speculate why the Pt/Pd catalyst shows a higher open cell potential than the Pt or Pt/Ru catalyst. Recall that formic acid electrooxidation occurs via the two reaction pathways described in the introduction: a direct oxidation pathway (reaction 1) and a reactive CO intermediate pathway (reactions 2–4). Now consider what happens at potentials close to that of a dynamic hydrogen electrode. Fig. 2 shows that at potentials of less than 0.3 V with respect to DHE, the current is much higher with Pt/Pd than with Pt or Pt/Ru. Yet Fig. 7 shows that the rate of CO stripping from the surface is negligible, i.e. the rate of reaction 4 is small. Clearly, current is being produced on the Pt/Pd catalyst via a pathway that does not involve reaction 4. The CO pathway, reactions 2–4 will not produce significant current unless the rate of reaction 4 is significant. Therefore, we suggest that the steady-state current observed at low potentials with respect to DHE in Fig. 2 cannot be associated with the CO pathway, and must be associated with reaction 1.

The opposite is true at potentials above 0.4 V with respect to DHE. Fig. 7 shows that the rate of reaction 4 is much higher on Pt/Ru than on Pt or Pt/Pd. Fig. 2 shows that at 0.5 V with respect to DHE the rate of formic acid electrooxidation increases sharply on Pt/Ru while no dramatic change is seen with Pt or Pt/Pd. Evidently, once reaction 4 starts on Pt/Ru, the current increases rapidly, so that Pt/Ru shows the highest current.

Our conclusion from the results in Figs. 2 and 7 are that reaction 1 shows an appreciable rate at low potentials with respect to DHE on Pt/Pd while the rate of reaction 4 shows an appreciable rate at moderate potentials with respect to DHE on Pt/Ru.

The results in Fig. 1 are consistent with this view. Notice that the Pt/Pd catalyst shows significant activity at cell potentials near the potential of H_2 (1.0 V in our fuel cell). Fig. 7 shows that the rate of reaction 4 is negligible at this potential, but still current is seen. These results again suggest that the reaction goes mainly via reaction [1] under real fuel cell conditions.

The one observation that we do not understand at present is that while Pt/Pd is better than Pt in accordance with our previous results [17], the effect is smaller than reported previously [17]. We observe a factor of 4 enhancement in current at 0.2 V with respect to DHE in a real fuel cell, while our previous work, done by depositing palladium on platinum nanoparticles in an electrochemical cell, found a factor of 80 enhancement. The Pt catalyst showed activity similar to that reported previously, but the Pt/Pd had a reduced activity on the membrane electrode assembly. Evidently, the process of making a catalyst ink and depositing it onto the MEA reduced the specific activity of Pt/Pd by a factor of 10–20. Clearly, more work is needed to find how to avoid this decrease in activity.

5. Conclusions

In summary the Pt/Pd anode catalyst gave an open circuit potential of 0.91 V, and showed significant current densities at cell potentials above 0.5 V. By comparison, the Pt/Ru

anode and showed a low open cell potential, but produced the most current at cell potentials below 0.3 V. By comparing the anode polarization and CO stripping experiments, Pt/Pd enhances cell activity by promoting the direct electrooxidation of formic acid (reaction 1) while the Pt/Ru catalyst operates mainly by the CO mechanism (reactions 2–4).

Acknowledgements

The authors would like to thank Tom Barnard and Piotr Waszczuk for preparing the catalysts used in this work. This material is based upon work supported by the Defense Advanced Projects Research Agency under US Air Force grant no. F33615-01-C-2172. The catalyst used in this work was originally developed in a project supported by the Department of Energy under grant DEGF-02-99ER14993. Any opinions, findings, and conclusions or recommendations expressed in this publication are those of the authors and do not necessarily reflect the views of the Department of Energy, the US Air Force, or the Defense Advanced Projects Research Agency.

References

[1] C. Rice, R.I. Masel, P. Waszczuk, A. Wieckowski, Characteristics of direct formic acid fuel cells, in: Proceedings of the 40th Power Sources Conference, 2002, p. 254.
[2] C. Rice, S. Ha, R.I. Masel, P. Waszczuk, A. Wieckowski, J. Power Sources 111 (2002) 83.
[3] M. Weber, J.-T. Wang, S. Wasmus, R.F.J. Savinell, Electrochem. Soc. 143 (1996) L158–L160.
[4] C. Rice, S. Ha, R.I. Masel, A. Wieckowski, Fuel cells for micro power applications, in: Proceedings of the DARPA MEMS Program, Detroit, 2002.
[5] B.D. Bath, H.S. White, E.R. Scott, Anal. Chem. 72 (2000) 433.
[6] X. Xia, T.J. Iwasita, J. Electrochem. Soc. 140 (1993) 2559.
[7] B. Beden, C. Lamy, Spectroelectrochemistry, theory and practice, in: R.J. Cale (Ed.), Plenum Press, New York, 1988 (Chapter 5).
[8] A. Bewick, B. Pons, R. Clark, R. Hester, Heyden, vol. XII, Wiley, London, 1985 (Chapter 1).
[9] T.D. Jarvi, E.M. Stuve, fundamental aspects of vacuum and electrocatalytic reactions of methanol and formic acid on platinum surfaces, in: J. Lipkowski, P.N. Ross (Eds.), Wiley, New York, 1998 (Chapter 3).
[10] N. Markovic, H. Gaseiger, P. Ross, X. Jian, I. Villegas, M. Weaver, Electrochem. Acta 40 (1995) 91.
[11] R. Parson, T. VanderNoot, J. Electroanal. Chem. 257 (1988) 9.
[12] P.N. Ross, The science of electrocatalysis on bimetallic surfaces, in: J. Lipkowski, P.N. Ross (Eds.), Wiley, New York, 1998, p. 63.
[13] S. Swathirajan, Y.M.J. Milhail, Electrochem. Soc. 138 (1991) 1321.
[14] J.B. Goodenough, A. Hamnett, R. Manoharan, B.J. Kenndy, S.A. Weeks, J. Electroanal. Chem. 240 (1988) 133.
[15] E. Herrero, K. Fanaszczuk, A. Wieckowski, J. Electroanal. Chem. 361 (1993) 269.
[16] B.J. Kennedy, T. Hamnett, Electroanal. Chem. A. 283 (1990) 271.
[17] G.Q. Lu, A. Crown, A. Wieckowski, J. Phys. Chem. B 103 (1999) 9700.
[18] P. Waszczuk, T. Barnard, C. Rice, R.I. Masel, A. Wieckowski, Electrochem. Commun. 4 (2002) 732.
[19] Y.Y. Tong, H.S. Kim, P.K. Babu, P. Waszczuk, A. Wieckowski, E. Oldfield, J. Am. Chem. Soc. 124 (2002) 468–473.
[20] S. Ha, C. Rice, R.I. Masel, A. Wieckowski, J. Power Sources, in press.